JOURNAL OF MATERIALS SCIENCE 24 (1989) 321–327

Gels from a double alkoxide: $(BuO)_2$–Al–O–Si–$(OEt)_3$

J. C. POUXVIEL, J. P. BOILOT
Groupe de Chimie du Solide, Laboratoire de Physique de la Matière Condensée, Ecole Polytechnique, 91128 Palaiseau Cédex, France

NMR study (^{27}Al, ^{29}Si) of the double Si–Al precursor $(BuO)_2Al–O–Si(OEt)_3$ in alcoholic solution shows molecular associations resulting from acid–base interactions with $O \rightarrow Al\equiv$ bondings. Gels have been prepared in the H_2O, HO^iPr, $(BuO)_2Al–O–Si(OEt)_3$ ternary phase diagram for a large range of oxide concentrations. For all the compositions, the very fast hydrolysis of Al–OR groups leads to an amphoteric sol. Nevertheless, the gelation time is governed by the initial water concentration, showing that the hydrolysis of Si–OR groups is the rate-determining process for the gelation. The apparent activation energy is about 20 kcal mol^{-1}. The relative hardness of gels increases when increasing the precursor concentration. After drying, the oxide skeleton of the xerogel is relatively dense, but the open porosity remains high up to about 1000° C. At this temperature, samples turn into optically clear and dense glass-ceramics, formed of mullite crystallites in amorphous silica.

1. Introduction

During recent years, the sol–gel process from alkoxides has become an area of intense research because it allows glasses or ceramics to be obtained at low temperature with possible control of the structure at the molecular level. Indeed, it is generally assumed that the mixing of the precursors in the liquid phase leads to materials with a better homogeneity than those obtained by solid state reactions.

Nevertheless, alkoxides exhibit very different rates of hydrolysis or condensation (for example, silicon and aluminium precursors). Thus, gels or powders with very different scales of chemical inhomogeneity can be obtained [1–4] depending on the preparation procedure. In this context, we have previously shown that complex precursors with Al–O–Si linkages can be used to prepare gels, glasses or ceramics [5–7].

The polymerization of the $(BuO)_2Al–O–Si(OEt)_3$ precursor has also been studied in detail [8], by ^{29}Si, ^{27}Al NMR and small-angle X-ray scattering (SAXS). The mechanism of polymerization can be summarized as follows. First, the addition of water results in a rapid hydrolysis of the $-Al(OR)_2$ groups. At the same time a rapid condensation process with formation of Al–O–Al bondings takes place and leads, after several minutes, to clusters of about 2 nm in radius. Second, the condensation proceeds by a slow aggregation of clusters, chemically limited by the hydrolysis of the Si–OR groups, and characterized by a fractal dimension near to 1.8.

In this paper, we report the preparation of gels for different compositions in the ternary diagram H_2O, HO^iPr, $(BuO)_2Al–O–Si(OEt)_3$. Our results are concerned with the physical aspect, the gelling time, the hardness of the gels and the structure of the gels under heat treatment.

2. Precursor structure

The crude formula of the aluminium–silicon ester is $(OBut)_2Al–O–Si(OEt)_3$ (Dynamit Nobel) but as observed for aluminium alkoxides [9], molecular associations with dimer, trimer, tetramer built around tetrahedral or octahedral aluminium atoms must be expected.

2.1. Al NMR study

^{27}Al NMR spectrum of the precursor (Fig. 1a) shows two resonances: a sharp peak ($\Delta\nu$ = 270 Hz) at 0 p.p.m., characteristic of octahedral aluminium atoms in a symmetrical site and a broad band ($\Delta\nu$ = 5000 Hz) at 50 p.p.m. indicating the presence of tetrahedral aluminium atoms. The ratio between the surfaces of the two peaks (Al^{IV}/Al^{VI}) is 6,

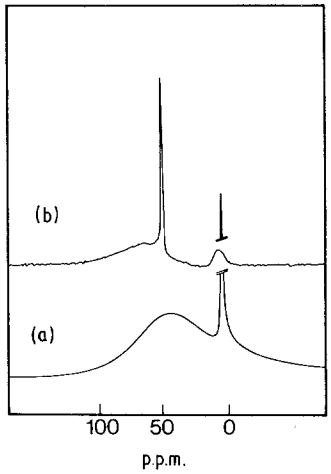

Figure 1 104 MHz-^{27}Al NMR spectra of the double alkoxide $(BuO)_2Al–O–Si(OEt)_3$ (p.p.m. from $Al(H_2O)_6^{3+}$), (a) in ^iPrOH, (b) after addition of water (the H_2O/precursor molar ratio is equal to 10).

0022–2461/89 $03.00 + .12

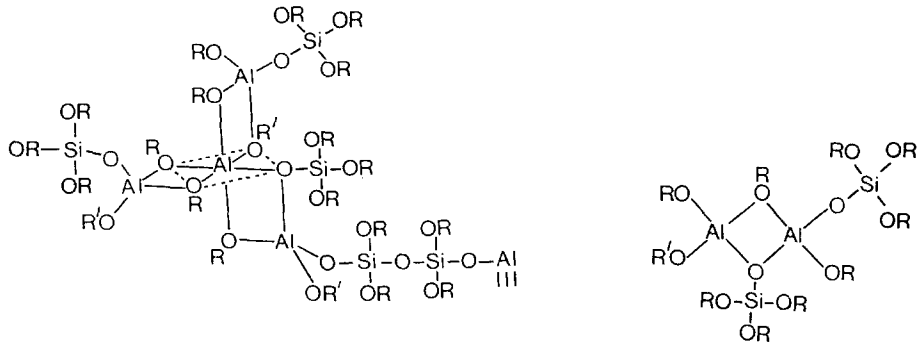

Figure 2 Proposed structures of molecular associations for the double alkoxide $(BuO)_2Al–O–Si(OEt)_3$.

and assuming the smallest size for the association, the solution can be seen as an equal distribution of tetramers and dimers (Fig. 2).

The addition of water, in order to obtain a water/precursor molar ratio equal to 10, involves a drastic and rapid change in the ^{27}Al NMR spectrum (Fig. 1b). The disappearance of the sharp band in the octahedral position is followed by the emergence of a new one at 49.4 p.p.m. ($\Delta\nu$ = 150 Hz) which corresponds to four-coordinated aluminium atoms in a very symmetrical site. These changes observed in the NMR spectra correspond to important modifications around aluminium atoms resulting from the hydrolysis of the Al–OR groups.

2.2. Si NMR study

The ^{29}Si NMR spectrum of the precursor under the same conditions (Fig. 3) shows several peaks corresponding to silicon atoms with different second neighbours. This spectrum does not change on using the proton decoupling technique and four groups of resonance can be distinguished. The first, A, and the second, B, are formed of four peaks separated by 1 p.p.m., and centered, respectively, at −84.6 and at −89 p.p.m. with respect to TMS used as the ^{29}Si chemical shift reference. The third, C, and the fourth, D, are formed of three peaks separated by 1 p.p.m. and centered, respectively, at −91.3 and at −95.8 p.p.m. The spectrum seems to be the addition of an initial spectrum (A + C) and the same translated spectrum (+4.5 p.p.m.) (B + D) with a different total intensity.

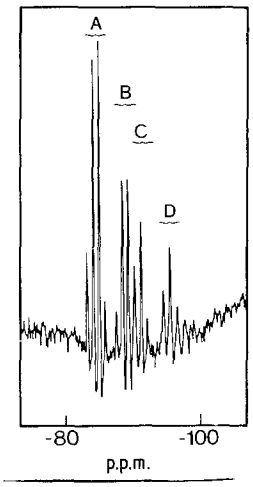

Figure 3 80 MHz-^{29}Si NMR spectrum of the pure double alkoxide $(BuO)_2Al–O–Si(OEt)_3$.

The addition of 10 mol water per mole precursor provokes the instantaneous disappearance of this second spectrum (B + D). The internal structure of each set can also be modified by heating the precursor, under reflux, in ethanol or butanol. With ethanol, the ratios between the peak intensity change, and we observe an increasing concentration of the species with the smallest chemical shift (in absolute value). The reverse effect is observed with butanol. This indicates, in agreement with previous observations on the $Si(OC_2H_5)_4$–propanol mixture [10], that these small changes in chemical shift are due to ester exchanges between OEt and OBu groups.

These preliminary experiments allow us to make the following assignments (Table I).

1. The first group A is due to Q^1 silicon with one Si–O–Al type bonding. The four peaks correspond to the four possibilities to choose the three remaining bondings with OEt and OBu groups and the intensities of the peaks indicate that the probabilities are almost equal.

2. The third group C can be attributed to Q^2 silicon with one Si–O–Al and one Si–O–Si type bonding on the basis that the chemical shift between set A and set C is the same as between Q^1 and Q^2 units in pure silica systems. The three peaks can also be explained by ester exchanges on the two remaining bondings.

3. The disappearance of sets B and D with the addition of water, their similarity with A and C, and molecular associations observed on ^{27}Al NMR suggest that these resonances probably arise from silicon atoms equivalent to those of set A and C but connected to aluminium atoms in different ways, for instance through one oxygen atom participating in an

TABLE I ^{29}Si chemical shifts given in p.p.m. with respect to TMS

$=Al–O–Si^*(OEt)_x(OBu)_{3-x}$	$x = 0$	−86.3
	$x = 1$	−85.3
	$x = 2$	−84.3
	$x = 3$	−83.3
$=Al–O–Si^*(OH)(OEt)_x(OBu)_{2-x}$	$x = 0$	−82.4
	$x = 1$	−81.4
	$x = 2$	−80.4
$=Al–O–Si–O–Si^*(OEt)_x(OBu)_{2-x}$	$x = 0$	−92.5
OAl=	$x = 1$	−91.5
	$x = 2$	−90.5
$=Al–O–Si–O–Si^*(OH)(OEt)_x(OBu)_{1-x}$	$x = 0$	−89.0
OAl=	$x = 1$	−88.0

TABLE II Gels in the H_2O–HO^iPr–$(BuO)_2Al$–O–$Si(OEt)_3$ diagram

Volumic composition	H_2O/Al–O–Si–, H	Concentration, C (mol l^{-1})	Gel time (h)	Hardness, $d = P/r^2$ (arb. units)
a 2.4.1	40	0.396	8	0.8
b 4.12.3	26	0.438	11	4
c 1.4.1	20	0.463	12	10
d 1.8.2	10	0.505	24	7
e 1.16.4	5	0.529	50	3
f 1.8.4	5	0.855	28	24
g 1.4.4	5	1.23	24	9
h 1.2.4	5	1.58	21	170
i 4.16.1	80	0.138	16	0.2
j 1.4.8	2.5	1.7	65	–
k 1.4.2	10	0.79	14	31
l 1.2.4	5	1.58	21	170
m 1.3.6	3.33	1.66	32	150
n 1.3.3	6.66	1.19	20	90
p 2.6.3	13.3	0.75	10	19
q 4.12.3	26.6	0.49	11	4
r 1.2.2*	10	1.11	16	23
t 1.1.1†	20	0.92	16	210
u 2.1.2†	20	1.11	5	1000
v 3.2.3†	20	1.04	7	1000
w 1.0.4†	5	2.22	8	400

*Compositions in zone III.
†Compositions in zone IV.

Al–O → Al bridge. These structures related to the molecular association would be destroyed by the addition of water and the rapid hydrolysis of the Al–OR groups.

3. Phase diagram

3.1. Preparation

Many compositions in the H_2O–HO^iPr–$(BuO)_2Al$–O–$Si(OEt)_3$ system have been prepared. A mixture of isopropanol and water is slowly poured into a mixture of precursor and isopropanol. The water contains HCl, used as a catalyst, in order to incorporate a constant quantity of protonic species (6.3×10^{-4} mol l^{-1}) to the organic solution. Samples were kept in sealed glass containers at 20° C.

The prepared compositions are summarized in Table II. Compositions are represented by points in the ternary diagram using the $x.y.z$ notation in which x, y, z are the volumic fractions of the species in the initial mixture. For example, 1.4.2 (see point k on Fig. 4) corresponds to the composition with one volume of water, four of solvent and two of precursor.

Gel time (t_g) was decided when observing the absence of flow after tilting the container. The relative hardness of the gels was tested with a conical metal piece loaded with P = 40, 100 or 500 g for 20 sec. The diameter of the indent, r, was measured under a lens and the results expressed in $d = P/r^2$ to compare the hardness of the gel.

The precursor concentration, C, the hydrolysis molar ratio $H = H_2O/Al$–O–Si, the gel time and the hardness are shown in Table II. After a long period of ageing ($> 20\, t_g$), the gels were dried at 120° C in the open container.

3.2. Gelation domain

Fig. 4 shows the results of the preparations. According to the physical aspect of the preparations, four zones

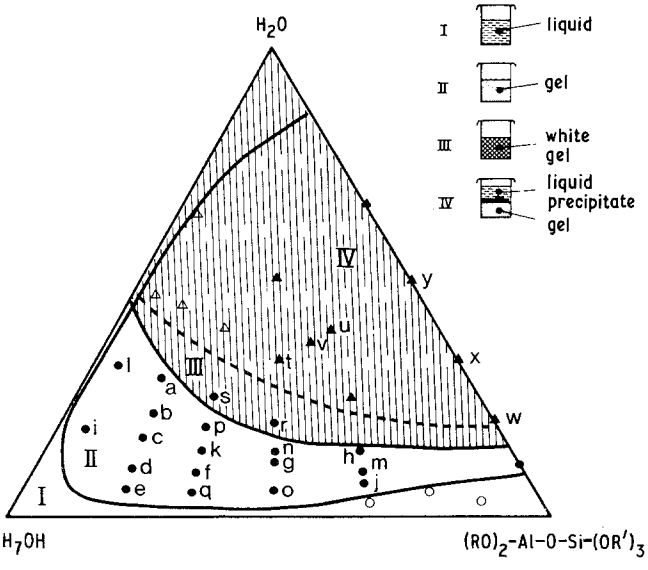

Figure 4 Gelation in the $H_2O/^iPrOH/(BuO)_2Al$–O–$Si(OEt)_3$ ternary phase diagram. The points correspond to compositions noted $x.y.z.$ for which x, y, z are the volume fractions of the species in the initial water/alcohol/precursor mixture (see Table II).

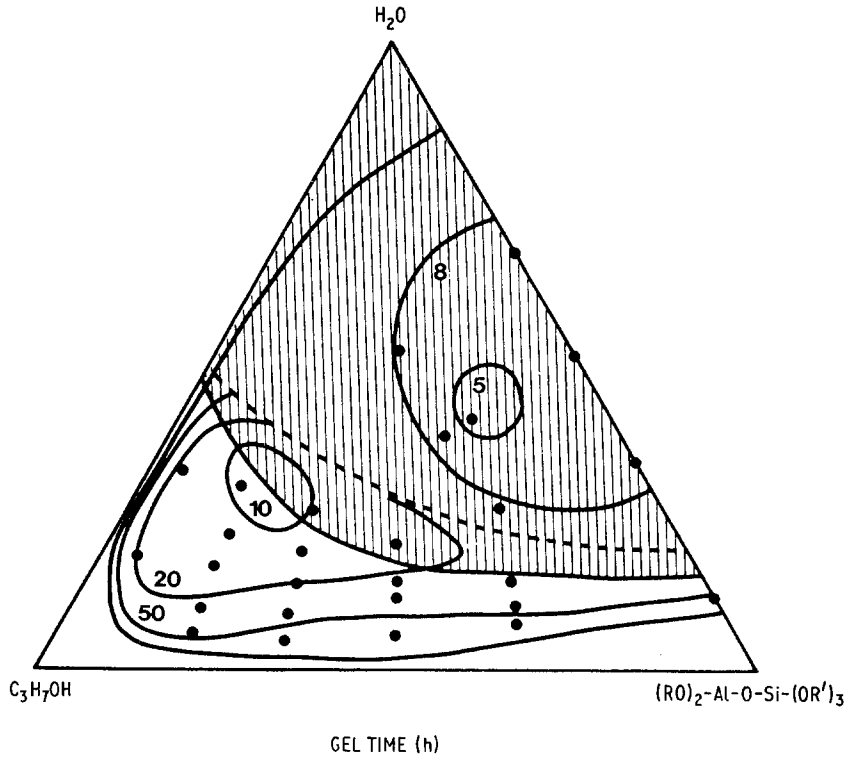

Figure 5 Isochronic curves for the gelation in the $H_2O/^iPrOH/(BuO)_2Al–O–Si(OEt)_3$ ternary phase diagram.

can be distinguished:

zone I, no gelation has been observed after 3 months and the solution remains clear;

zone II, the addition of water gives rise to cloudy white precipitates in the solution which dissolve quite rapidly on stirring. After several hours, the solution develops into monolithic and transparent gels;

zone III, as water is added, the same behaviour is observed but the liquid turns white before the gel point is reached. Monolithic but white and opaque gels are obtained;

zone IV, after addition of water, a phase separation is observed and precipitation occurs. After several hours the solution is divided into two parts: the bottom is a clear solution which turns into a clear and monolithic gel and the top is constituted with a liquid in which some powder is suspended. The mass ratio of gel over precipitate may range from 0 to 100%. The phase separation is clearly related to the composition of the solvent (water + propanol) and corresponds to a loss of solubility of the polymer into the initial solvent. The upper liquid contains both water and propanol.

4. Gelation time

Fig. 5 shows the isochronic curves for the gelation of the various compositions in the ternary diagram. When the gelation occurs, the gel time is less than 200 h which is a short time in comparison with that observed for the pure silica system (up to 200 days).

4.1. Homogeneous domain (zone II and III)

The shortest gelation time of about 8 h is obtained for the composition 2.4.1 which has a low precursor concentration (0.4 mol l^{-1}) and contains a large amount of water (H = 40) corresponding to eight times the quantity required to hydrolyse all the organic groups.

4.1.1. Influence of the water/AlOSi hydrolysis molar ratio (H)

For a constant concentration of the precursor, C = 0.5 mol l^{-1}, the decrease of the molar ratio $H = H_2O$/Al–O–Si from 40 down to the stoichiometric value for total hydrolysis (H = 5) leads to an increase in the gel time from 8 up to 50 h. At higher precursor concentration, C = 1.6 mol l^{-1}, a smaller amount of water can be added without precipitation but we observe a more important variation of the gel time (three times shorter when H decreases from 5 down to 2.5). Finally, the gelation is not observed for an H value less than 2.

4.1.2. Influence of the precursor concentration (C)

At a low ratio H = 5, the gel time only increases from 21 to 28 h when the precursor concentration changes from 1.58 to 0.86 mol l^{-1}, but it reaches 50 h or decreases to 8 h when the precursor concentration is 0.528 and 2.22 mol l^{-1}, respectively. For H = 10, the

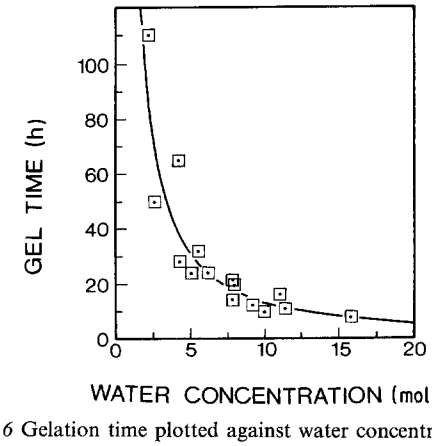

Figure 6 Gelation time plotted against water concentration in the initial mixture.

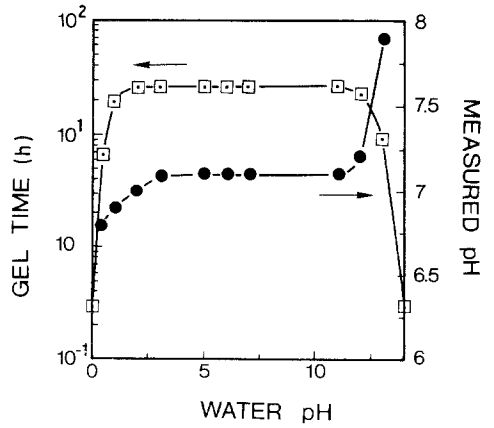

Figure 7 pH of the solution and gel time for the 1.4.2 composition (point k on Fig. 4) as a function of the pH of the water added in the initial organic mixture.

same variation of the gel time with respect to the precursor concentration is observed unless the precipitation occurs during gelation (compare 1.8.2 and 1.4.2 with 1.2.2 which is localized in zone III).

These results show that the precursor concentration and the hydrolysis ratio are cooperative factors in the gelation kinetic. Nevertheless, the comparison between the concentrated composition 1.4.8 ($C = 1.7\,\text{mol}\,l^{-1}$, $H = 2.5$ and $t_g = 65\,h$) and diluted one 4.16.1 ($C = 0.138\,\text{mol}\,l^{-1}$, $H = 80$ and $t_g = 16\,h$) suggests that the main parameter for the gelification is the water concentration (H^*C). In fact, if we plot the gel time against the water concentration (H^*C) for all the compositions with H more than 5 and whatever the value of C (Fig. 6), we find that the general trend is a decrease of the gelation time as the water content increases.

4.1.3. pH and temperature effects

The composition 1.4.2, i.e. $H = 10$, $C = 0.79\,\text{mol}\,l^{-1}$, has been prepared by varying the pH of the added water from 0 to 14. Fig. 7 shows the variations of the pH of the solution, measured with a glass electrode, and of the gelation time with the pH of the water. Whatever the pH of the water in the range 2 to 12, the pH of the solution remains approximately constant (about 7), in agreement with the amphoteric behaviour of the aluminium hydroxides, and no significant change of the gel time is observed. Moreover, the addition of water provokes the appearance of white clouds which dissolve quite rapidly after vigorous stirring and the solution gives optically clear monolithic gels.

For pH values below 2 or above 12, significant variations of the pH of the solution are observed. The polymerization is then catalysed by H^+ or OH^- ions and the solution gelatinizes very rapidly. However, the final gel is generally white and opaque.

The temperature effect has been studied on three compositions, obtained by dilution of 1.4.2, which exhibit the same concentration of the precursor ($C = 0.40\,\text{mol}\,l^{-1}$) and three different values of H: 10, 20 and 30. In each case, the variations of the gelation time with the temperature can be represented by an Arrhenius law: $1/t_g = A \exp -E/RT$, in which the apparent activation energy, E, is equal to 20 kcal mol^{-1}. Indeed, in agreement with the water concentration dependence of the gelation time, t_g is governed primarily by the hydrolysis and this value of E is probably related to the hydrolysis of Si–OR groups which is the rate-determining process. Moreover, the activation energy is constant for the three values of H, indicating no significant change of the polymerization mechanism as a function of the water concentration.

4.2. Phase separation domain (zone IV)

In this domain, it is obviously difficult to know the real influence of the H and C parameters on the gelation.

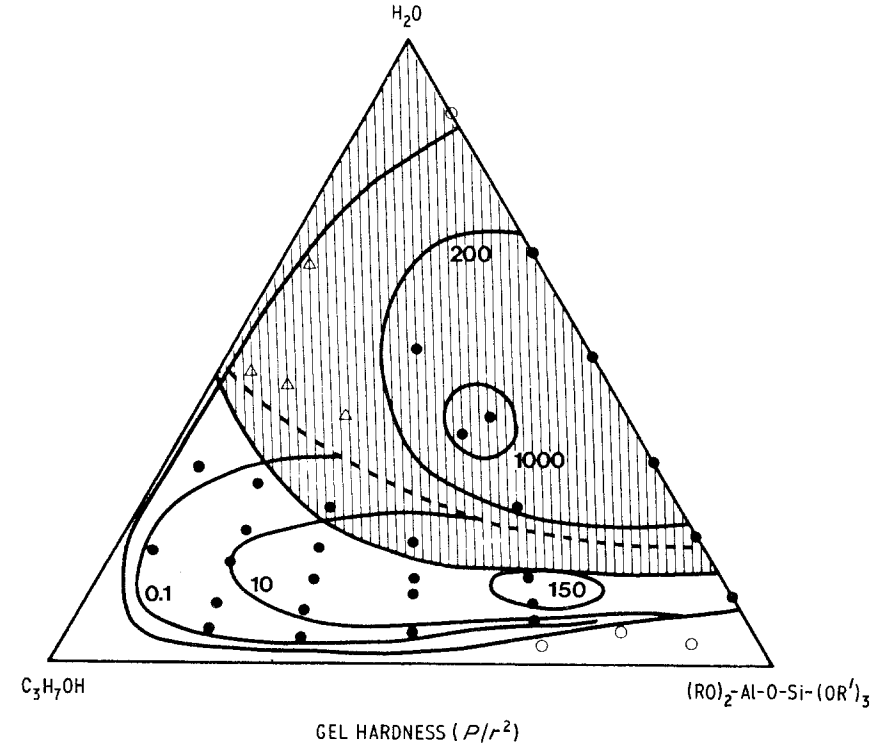

Figure 8 Relative hardness for gels in the $H_2O/^iPrOH/(BuO)_2Al–O–Si(OEt)_3$ ternary phase diagram.

However, the gel time of the bottom phase does not clearly depend on the composition because all these solutions have approximately the same gelation time (8 h). The shortest gel time (5 h) and the longest (16 h) are observed for the 2.1.2 and the 1.1.1 compositions, respectively. pH and temperature effects are close to those observed in the homogeneous domain.

5. Gel hardness

Fig. 8 shows the hardness of the gels in the phase diagram estimated using the indent method.

5.1. Homogeneous domain

The hardest gels (d = 170) are obtained for H = 5 near the composition 1.2.4 which has a small amount of water and a high precursor concentration. As the dilution increases, the hardness falls off very rapidly (Table II) in spite of higher H values. The gel compositions with shortest gelation time are relatively soft (d = 1). For low concentrations $C = 0.5\,\text{mol}\,l^{-1}$, there is no direct correlation between d and H or t_g because the hardness goes through a relative maximum of d = 10 for H = 20 and decreases down to 3 for H = 5 or down to 0.8 for H = 40 (Table II). Water content and precursor dilution are competing factors.

5.2. Phase separation domain

Only the bottom gels, which represent a sufficient proportion of gel with respect to powder precipitate, have been tested. In spite of equivalent gelation time, relative hardnesses are quite different and range from 200 to 1000 but they are obviously higher than in the other domain. Here, the shorter gel time, the harder the gels become (Table II).

The hardness of the gels is related to the density of Al–O–Si and Al–O–Al bondings and to the structure connectivity. In the homogeneous domain, the maximum of the hardness is observed for gels obtained from the solutions prepared with high concentration of organic precursor (Fig. 9) and with, at least, a stoichiometric concentration of water. In the heterogeneous domain, the phase separation increases the concentration of the precursor in that part of the solution which gelatinizes, and therefore, gels are characterized by a high hardness.

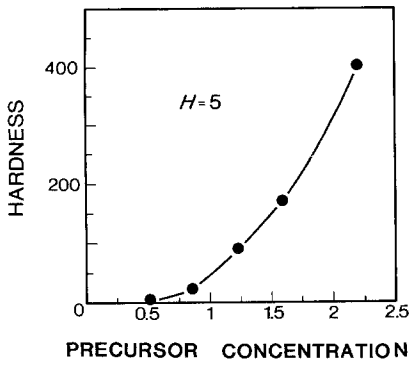

Figure 9 Relative hardness plotted against the precursor concentration for the initial H_2O/precursor molar ratio equal to 5.

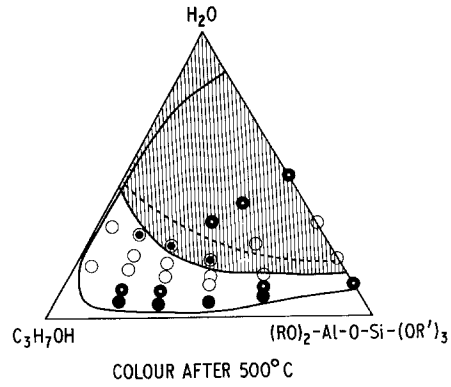

Figure 10 Colouration of xerogels after heating at 500° C: (●) brown, (◉) yellow and transparent, (⊙) white and opaque, (○) colourless and transparent.

6. Thermal treatment

6.1. Xerogel colouration

After firing at 500° C, the colouration of the gels (Fig. 10) qualitatively informs about the carbon formation in the gel structure due to the incomplete removal of inorganic groups. In the homogeneous domain, by increasing the concentration of water in the initial mixture, xerogels evolve from a brown colouration to a yellow one, then become colourless and transparent. In the heterogeneous domain, the reverse behaviour seems to take place. In fact, the phase separation changes the effective water concentration and probably a high initial water concentration accelerates the phase separation and therefore decreases the number of hydrolysed Si–OR groups. Obviously, these results show that a total hydrolysis of the organic groups is required to obtain an optically clear xerogel.

6.2. Drying and thermal evolution

Gelation and drying of gels prepared from the 1.4.2 composition have been performed in different ways.

(a) Gels denoted A have been prepared by sol concentration in an open container.

(b) Gels denoted B have been prepared in a closed container and different drying methods have been used (drying at 70° C after opening the container, very slow drying at 20° C with holes in the stopper, dipping in acetone and drying at 20° C in the open container after removal of the liquid solvents).

The apparent density and the open porosity of the xerogels have been measured by Archimedes method in cyclohexane and oil (density 0.882). In fact, whatever the drying process, the open porosity of the gels B is about 60%. In contrast, for gels A, in which a partial removal of organic groups takes place before the gel point, the porosity is only 30%. Finally, for both types of gel, the apparent density is the same: $1.9\,\text{g}\,\text{cm}^{-3}$, corresponding to a relatively dense skeleton formed of Si–O–Al and Al–O–Al bondings.

After drying, thermal treatment of xerogels has been performed for the two types of gels by heating at $100°\,\text{C}\,\text{min}^{-1}$ up to the final temperature and holding 2 h before cooling (short cycle). Fig. 11 shows the temperature dependence of the apparent density and of the open porosity for the two types of gels (A and B).

The differences observed between the A and B

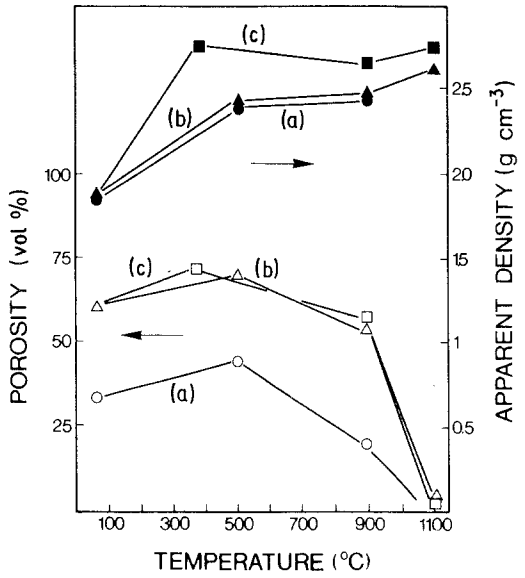

Figure 11 Temperature dependence of the porosity and of the apparent density for gels prepared from the 1.4.2 initial mixture after different drying and firing processes. (a) With removal of volatiles during the gelation and short firing time. (b) Without removal of volatiles during the gelation and short firing time. (c) Without removal of volatiles during the gelation and long firing time.

xerogels at 100° C remains up to 900° C. The porosity increases in the range 350 to 500° C. This increase can be related to the pyrolysis of organic radicals and to the departure of OH groups on pore surfaces. At 900° C, no densification is noted and the xerogel is clear and transparent. The open porosity only disappears (< 5% after 1100° C) with the partial crystallization of mullite which has been previously displayed at 985° C by DTA and X-ray diffraction [5]. As a consequence, the shape of the sample becomes very irregular but the sample is still transparent.

A long thermal cycle, with the same heating rate, but with a step of 24 h at 360° C and 2 h at the final temperature, has also been performed on gels B. The curves of apparent density against temperature (Fig. 11) exhibit significant differences for the two firing cycles (short and long): For the long cycle, it reaches 2.75 g cm^{-3} at 360° C (95% of the theoretical density calculated from a mixture of amorphous silica and mullite) and remains virtually at this high value at higher temperature. For the short cycle, the apparent density is 2.45 g cm^{-3} at 500° C and only reaches 2.65 g cm^{-3} at 1100° C. These results demonstrate that the long treatment at 360° C allows subsequent condensation reactions with the departure of water, such as:

$$\text{Si–OR} + \text{Al–OH} \rightarrow \text{Si–O–Al} + \text{ROH}$$

$$\text{Si–OH} + \text{Al–OH} \rightarrow \text{Si–O–Al} + \text{H}_2\text{O}$$

These condensations facilitate the elimination of the close porosity by giving a certain flexibility to the network. At higher temperature, the stiffness of the structure prevents the elimination of defects, such as small pores, which are confined in the network. These reactions do not play any role in the elimination of the macroscopic porosity, which suggests that the structure of the xerogel at 100° C is already rigid.

7. Conclusion

NMR results indicate that the structure of the $(BuO)_2Al–O–Si(OEt)_3$ precursor in alcoholic solution is complex, molecular associations leading to dimer and tetramer through Al–O → Al bondings. Moreover, a weak condensation on silicon atoms (dimeric units with Si–O–Si bonding) is displayed in the solution.

In the $H_2O/^iPrOH/(BuO)_2Al–O–Si(OEt)_3$ ternary phase diagram, we notice that gels can be obtained in a reasonable time (< 3 days) within a large range of water/precursor ratios ($2 < H < 100$) and consequently in a large range of oxide concentrations.

The gelation time decreases on increasing the water content. This clearly shows that the hydrolysis of the Si–OR groups is the rate-determining process for the cluster–cluster aggregation mechanism of gelation which is characterized by an "apparent" activation energy, E, of 20 kcal mol^{-1}. This reaction is obviously catalysed by protonic or hydroxyl species, but the amphoteric behaviour of the sol implies a large addition of acid or base to modify the pH.

The gel hardness is governed by the precursor concentration. The increase of the initial precursor concentration leads to high connectivity in the gel and therefore to a high relative hardness.

After gelation, the gel is formed of a rigid oxide skeleton and of large pores containing the solvent. By drying, the volatiles are removed and only a very small contraction of the network occurs. The open porosity remains high (up to 50% for 1.4.2 composition).

The thermal treatment at 400 to 500° C leads to the combustion of the remaining organic groups and consequently increases the open porosity and the apparent density. The complete densification only appears at 985° C, with a partial crystallization of mullite and the formation of a transparent glass–ceramic.

References

1. B. E. YOLDAS, *J. Amer. Ceram. Soc.* **59** (1980) 479.
2. D. W. HOFFMAN, R. ROY and S. KOMARNENI, *ibid.* **67** (1984) 468.
3. B. E. YOLDAS, *ibid.* **65** (1982) 387.
4. K. OKADA and N. OTSUKA, *ibid.* **69** (1986) 652.
5. J. C. POUXVIEL, J. P. BOILOT, A. DAUGER and L. HUBERT, in "Better Ceramics through Chemistry II", MRS meeting Palo Alto, edited by C. J. Brinker, D. E. Clark and D. R. Ulrich, Vol. 73 (Material Research Society, Pittsburgh, 1986) p. 269.
6. J. C. POUXVIEL and J. P. BOILOT, in "Ultrastructure Processing of Ceramics, Glasses and Composites", San Diego, February 1987, (Wiley, USA) in press.
7. J. C. POUXVIEL, J. P. BOILOT, O. PONCELET, L. G. HUBERT, A. LECOMTE, A. DAUGER and J. C. BELOEIL, *J. Non-Cryst. Solids* **93** (1987) 277.
8. J. C. POUXVIEL, J. P. BOILOT, A. LECOMTE and A. DAUGER, *J. Physique (Paris)* **48** (1987) 921.
9. O. KRIZ, B. CASENKY, A. LYCKA, J. FUSEK and S. HERMANEK, *J. Magn. Res.* **60** (1984) 375.
10. J. C. POUXVIEL, J. P. BOILOT, J. C. BELOEIL and J. Y. LALLEMAND, *J. Non-Cryst. Solids* **89** (1987) 345.

Received 15 July
and accepted 9 October 1987